Inverse Problems in Engineering: Theory and Practice
3rd International Conference on Inverse Problems in Engineering
June 13-18, 1999, Port Ludlow, WA, USA

IM03

A GENERALIZED APPROACH FOR ATOMIC FORCE MICROSCOPY IMAGE RESTORATION WITH BREGMAN DISTANCES AS TIKHONOV REGULARIZATION TERMS

Geraldo A. G. Cidade[1], Celia Anteneodo[1], Nilson C. Roberty[2] and Antônio J. Silva Neto[3,2]
[1]Instituto de Biofísica Carlos Chagas Filho - CCS/UFRJ, CEP 21949-900, Rio de Janeiro, RJ, Brazil, gcidade@biof.ufrj.br and celia@cbpf.br
[2]Nuclear Engineering Program - COPPE/UFRJ, CP 68509, CEP 21945-970, Rio de Janeiro, RJ, Brazil, nilson@lmn.con.ufrj.br.
[3]Instituto Politécnico, UERJ, CP 97282, CEP 28601-970, Nova Friburgo, RJ, Brazil, ajsneto@iprj.uerj.br.

ABSTRACT

Tikhonov's regularization approach applied to image restoration, stated in terms of *ill-posed* problems, has proved to be a powerful tool to solve noisy and incomplete data. This work proposes a variable norm discrepancy function as the regularization term, where the entropy functional was derived. Our method is applied to true Atomic Force Microscopy (AFM) biological images, producing satisfactory results. These images represent a mapping of local interaction forces exerted between a reduced scaled AFM sensing tip and the biological sample, kept alive in aqueous or air enviroment.

INTRODUCTION

The Atomic Force Microscopy (AFM) technique (Binnig et al., 1986) consists, basically, on the production of force images, formated like tridimensional photographs, by means of very small sensing tips, used to map the interaction between the sample and the tip. The greatest advantage of the AFM technique is its ability to image the surface of randomly distributed macromolecules *in situ*, if not in *vivo*, which opens a new promising approach in the structural biology field (Glaeser, 1994), complementing well with other techniques such as electron-microscopy and X-ray diffraction. Among several powerful capabilities, the AFM technique, when applied to biological samples, allows the visualization of microscopic structure features from cell membrane surfaces, like proteins, in the nanometer range (Amato, 1997; Oberleithner et al., 1994). For images in this range scale, the interaction between the tip an the sample can produce blurred images, with the blurring being related to the tip geometry (operator). Besides the blurring effect, additive noise is also present. Being an *ill-posed* problem, a direct inversion is not directly applied to deconvolve the blurred image.

The solution of *ill-posed* problems, by means of regularization (Tikhonov and Arsenin 1977), resulted in a substantial number of developments in different application fields, such as astronomy (Gull and Daniell, 1978) and scanning-tunneling microscopy (Kokaram et al., 1995). For the solution of any direct problem, three essential requirements have to be satisfied: *existence*, *uniqueness* and *stability*. Depending strictly on the quality of the operator in presence of noise, at least one of these qualifiers may not be met on the formulation of inverse problems. The regularization theory applied to image restoration is based on the trade-off between fidelity to the data and smoothness of the solution in the space domain, converting an *ill-posed* problem into a *well-posed* one (Kang and Katsaggelos, 1995), deriving an acceptable approximation towards the most feasible solution (original image).

MATHEMATICAL FORMULATION OF THE DIRECT AND INVERSE PROBLEMS

When the operator intrinsically exhibits geometrical limitations, as is the case of the cantilever's tip used in AFM to produce sample scanning images in the nanometer range, considerable blurring effects (tip-to-sample convolutions) may occur. Also due to the extremely small scale, other undesirable additive perturbations (noise) could lead to images with poor signal-to-noise ratios. Differently from image enhancement (Wu, 1997), the main goal in image restoration is to make the processed image to be as close to the true image as possible in regard to intensity distribution. Therefore, the effects of blurring and additive noise may be outlined as:

$$y = Bx + n, \qquad (1)$$

where $y \in \psi$ represents the real image, $x \in \Im$ the original image (being $\Im$ and ψ Hilbert spaces), B a compact operator, described by a point-spread function (PSF) matrix of the imaging system ($B: X \rightarrow Y$) and n the additive noise, generally of Gaussian type. Considering only the first term in the right hand side of Eq. (1), the image (without additive noise) is described by a Fredholm equation of the first kind (Kress,1989):

$$y(z) = \quad b(z,w)\varphi(w)dw \tag{2}$$

where $\varphi(w)$ represents the expected unique solution obtained along the restoration process, located near the primitive intensities in the domain region, in analogy to x in Eq. (1).

This problem is considered *well-posed* if, for each $y \in \psi$, a unique solution $x \in \Im$ does exist, depending continuously on the observed data, otherwise it would be *ill-posed* (Karayiannis and Venetsanopoulos, 1989), with no apparent solution if the B operator is a square matrix, with det(B)=0. Based on this argument, the inverse problem

$$x = B^{-1}y \tag{3}$$

was considered *ill-posed* by Franklin (1970). As the eigenvalues accumulate in zero (Tikhonov and Arsenin, 1977), a small perturbation yields a large perturbation in the solution (Kang and Katsaggelos, 1995). Therefore, the inverse problem is solved as a finite dimensional optimization problem in which we minimize a functional such as the one with the square residues

$$L(x) = \|y - Bx\|^2 \tag{4}$$

This is the well known least squares method.

TIKHONOV REGULARIZATION

The functional to be minimized may also be constructed based on the Bayesian argument of conditioned probability (Kokaram et al., 1995). Searching for an adequate compromise between accuracy and stability, a Tikhonov regularizing term is added to the norm given by Eq. (4)

$$Q(\hat{x}) = \|y(i,j) - \sum_{k=-N}^{N}\sum_{l=-N}^{N} b(k,l).\hat{x}(i+k, j+l)\|^2 - \alpha S \quad (a > 0; i, j = 1,2,\ldots, M) \tag{5}$$

generating a regularized solution to this problem (Mohammad-Djafari and Demoment, 1985), based on the classical Tikhonov regularizing functional (Kress, 1989), where *y(i,j)* represents the acquired image, *b(k,l)* the PSF, $\hat{x}$ the estimated data that we want to determine, and αS the regularization term, where parameter α determines the trade-off between the accuracy and the stability of the solution; *(i,j)* is a specific pixel of the total M x M image pixels, and the blurring discrete operator *b(k,l)* convolves (2N+1) x (2N+1) pixels around that specific pixel. Depending on the image characteristics, the functional S can be defined by any prior function that imposes no correlation on the image for which there is no evidence in the available data (maximally noncommittal).

Although other general functionals can be used (Anteneodo and Plastino, 1999), like the Csiszer's measure (Kapur and Kesavan, 1992), this work proposes another functional, which we call *q-discrepancy*, to derive a family of regularizing terms using Bregman distances of convex projections

$$S = D_q(\hat{x}, \bar{x}) = \frac{1}{1+q}\sum_{p=1}^{M\times M}\left\{ \hat{x}_p \left| \frac{(\hat{x}_p)^q - (\bar{x}_p)^q}{q} \right| - (\bar{x}_p)^q(\hat{x}_p - \bar{x}_p) \right\} \tag{6}$$

with non-negative q, from where the modified cross-entropy functional

$$S = \sum_{i=1}^{M}\sum_{j=1}^{M}[\hat{x}(i,j) - \bar{x}(i,j) - \hat{x}(i,j)\ln\frac{\hat{x}(i,j)}{\bar{x}(i,j)}] \tag{7}$$

is obtained as a particular case when $q \rightarrow 0$, where $\hat{x}(i,j)$ represents the estimated image data values, $\bar{x}(i,j)$ describes a prior reference model, being the latter stated in terms of the weighted average from the acquired image data. The functional Q, given by Eq. (5), will be minimized when both the squared residues, given by Eq. (4), and discrepancies tend to be minimal (maximal configurational entropy); the *maximum entropy* criterion, proposed by Jaynes (Kapur and Kesavan, 1992), applied to image restoration by Frieden (1972), establishes that "*of all feasible (possible) solutions, there should be used the one that has the maximum configurational entropy"* (Wu, 1997).

In order to minimize the Q functional we make $\partial Q / \partial \hat{x} = 0$, yielding a system of non-linear equations

$$\begin{aligned}
&F_1(x_1, x_2, x_3, \ldots\ldots, x_{M\times M}) = 0\\
&F_2(x_1, x_2, x_3, \ldots\ldots, x_{M\times M}) = 0\\
&F_3(x_1, x_2, x_3, \ldots\ldots, x_{M\times M}) = 0\\
&\ldots\ldots\ldots\ldots\ldots\ldots\ldots\ldots\ldots\ldots\\
&F_{M\times M}(x_1, x_2, x_3, \ldots\ldots, x_{M\times M}) = 0
\end{aligned}$$

where MxM=65536 (each row represents the whole image), for an image of 256 x 256 pixels. To solve this system we use the multivariable Newton-Raphson method, in which a linearization is obtained using the Taylor expansion, keeping only the first order terms. Making use of such procedure, corrections of the unknowns can be obtained iteratively, using the Gauss-Seidel method (Wu, 1997):

$$\Delta \hat{x}_{rs}^{c+1} = -\frac{1}{\left.\frac{\partial F_{rs}}{\partial \hat{x}_{rs}}\right|^{c}} \left[F_{rs} + \sum_{\substack{m=1 \\ m\neq r}}^{M} \sum_{\substack{n=1 \\ n\neq s}}^{M} \frac{\partial F_{rs}}{\partial \hat{x}_{mn}} . \Delta \hat{x}_{mn} \right], \tag{8}$$

$$r, s = 1,2,\ldots, M, \qquad \Delta \hat{x}^{0} = 0$$

where **c** is the step iteration counter. The Newton Raphson estimates are obtained with

$$\underset{\sim}{\hat{x}}^{(c+1)} = \underset{\sim}{\hat{x}}^{(c)} + \gamma . \Delta \hat{x}^{(c+1)} \tag{9}$$

where γ is used as a gain factor to produce more stability along the iterative process, as the convergence takes place towards the expected solution. Figure 1 illustrates the algorithm's flow chart, which uses the Q_{min} criterion to stop the process. The program was written in C language, using the C++ Builder Server/Client platform from Borland Inc., with a user friendly interface.

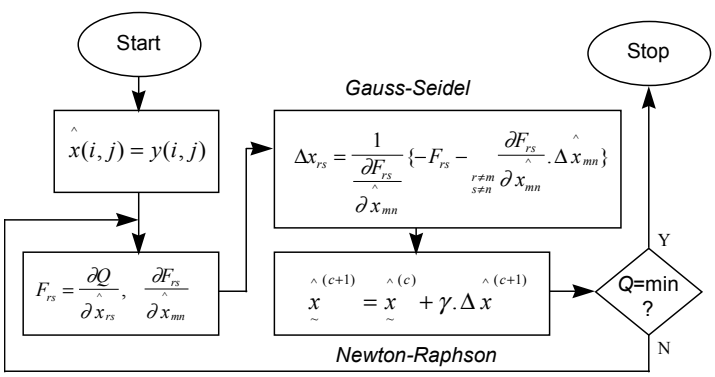

Figure 1. Image restoration algorithm.

RESULTS AND DISCUSSION

In our case, the cantilever's tip effects (blurring) present in the 256 x 256 AFM images can be clearly observed in dimensions less than or equal to 1μm x 1μm. For this reason, in this scale, postacquisition processing (image restoration) becomes necessary to reveal important specimen's structural and functional features. Both the regularization parameter α and the gain factor γ were adjusted to produce optimal restoration in the observer point of view. The mathematical representation of the tip geometry (blurring operator) was chosen to be similar to a Gaussian tridimensional distribution (Kokaram et al., 1995), with adjustable variance (σ^2). The cross-entropy functional, derived from the Bregman distance based on the *q-discrepancy* functional ($q \to 0$), was used in the regularization term.

Figure 2a illustrates a true 1μm x 1μm AFM biological image of an eritroblast in leukemia pathology, whose details were improved (Fig. 2b) after running the algorithm, assuming a 9 x 9 deconvolution Gaussian matrix (DGM) with σ^2 =10, using α=0.03 and γ=0.2.

Figure 3a shows another true 600 nm x 600 nm image of the same sample, restored with different Gaussian tip profiles (Figs. 3b and 3c), using the same α and γ values as in Fig. 2b. Figure 3b shows minor improvements in its contrast contents for a 9 x 9 DGM with σ^2 =10, whereas Fig. 3c reveals more visible contours after deconvolving the true image with a 15 x 15 DGM with σ^2 =40.

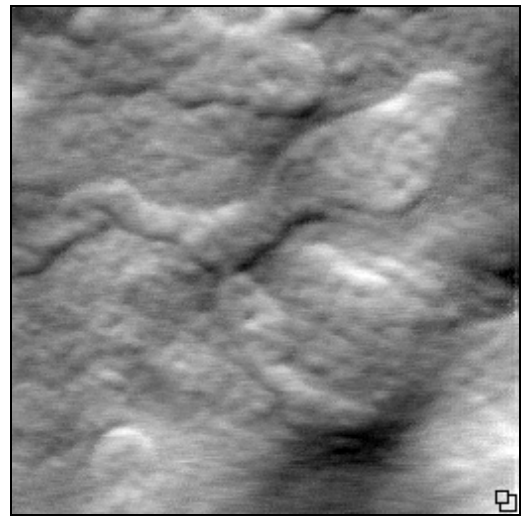
Figure 2a. AFM true 1μm x 1μm image of an eritroblast in leukemia.

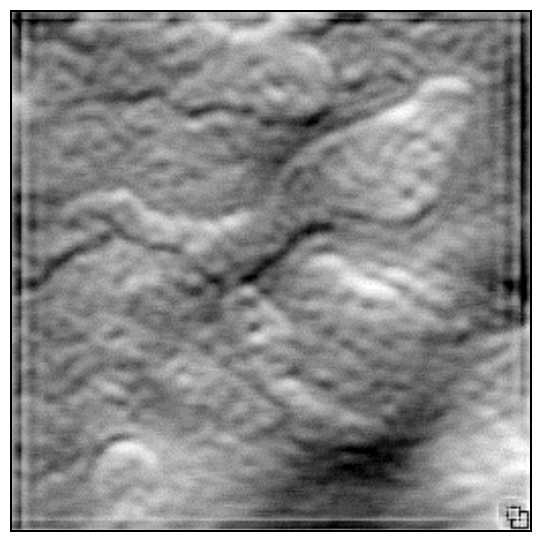
Figure 2b. Restored image using a 9 x 9 DGM (σ^2 =10), with α=0.03 and γ=0.2.

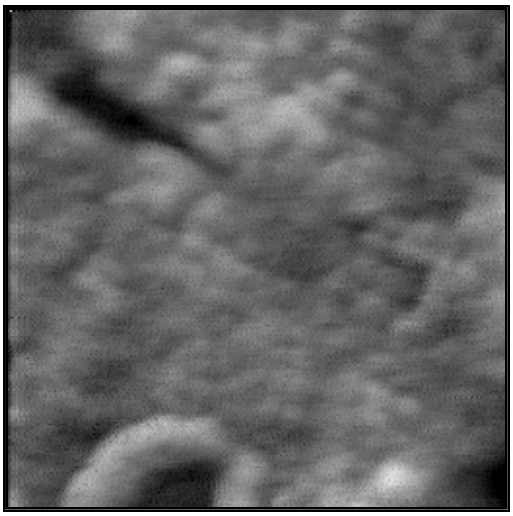

Figure 3a. AFM true 600 nm x 600 nm image of an eritroblast in leukemia.

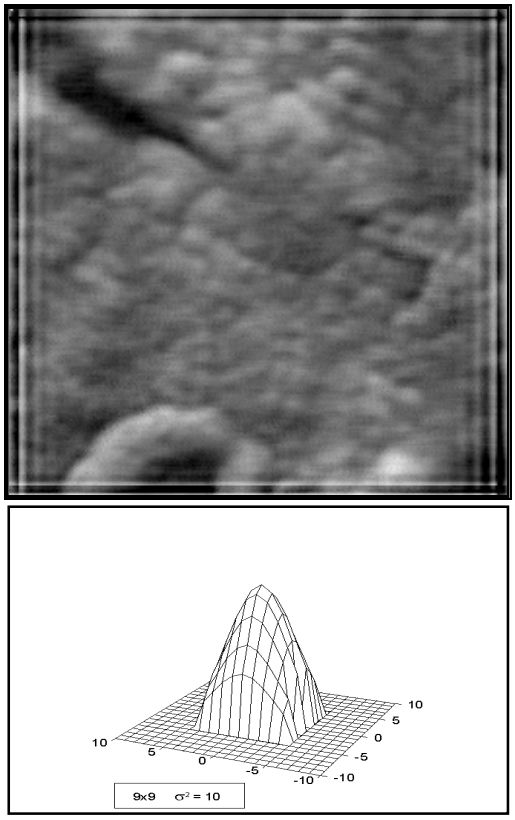

Figure 3b. Restored image using a 9 x 9 DGM (σ^2 =10), with α=0.03 and γ=0.2; tip geometry is shown bellow.

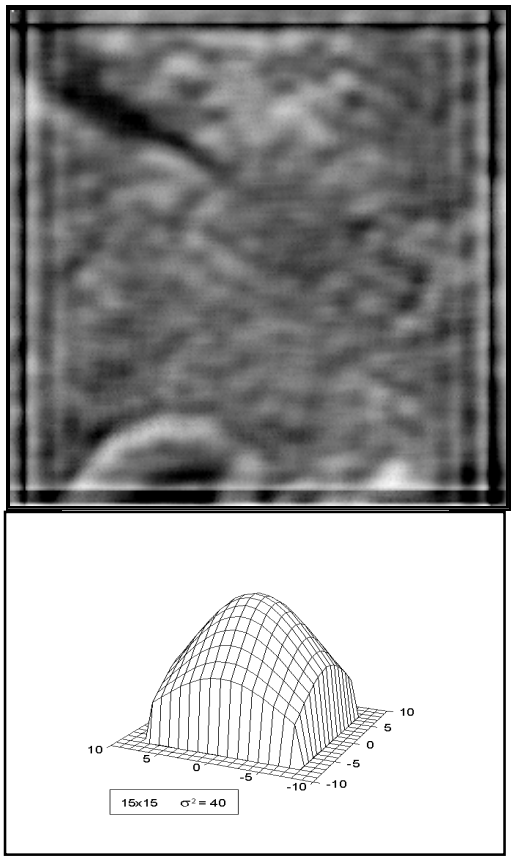

Figure 3c. Restored image using a 15 x 15 DGM (σ^2=40), with α=0.03 and γ=0.2; tip geometry is shown bellow.

We must stress that for the expert observer the structures added to the reconstructed images do not correspond to artifacts. They bring relevant contrast information that would be lost if other techniques, such as Fourier Transform (FFT), had been applied.

It can be noted that all restored images exhibit a false frame (border effect) due to the calculations made around the image border, by using values outside the image domain. We are working on the attenuation of such undesirable effect by reflecting the image's border values. We should emphasize that, as expected, the results obtained depend on the choice of parameter α. Therefore, the proper choice (determination) of α is an important aspect of the inverse problem here described.

CONCLUSIONS

The results obtained so far have been very encouraging. At the moment we are working on the implementation of a general regularization term based on the *q-discrepancy*. Our goal is to determine which value for *q* yields the best solution of the reconstruction problem.

With respect to the regularization parameter in Eq. (5), one comment is in order. The determination of an optimal parameter is possible, and has already been done for the squared residues norm (Kress, 1989), but is computationally involved. Therefore, the most common approach is to perform numerical experimentations for the estimation of such parameter (Kokaram

et al., 1995). The results presented in Figs. 2 and 3 were obtained applying this approach.

We have also in mind to develop and implement an automatic correction of the regularization parameter along the iterative procedure, that may improve the estimates.

ACKNOWLEDGMENTS

The authors acknowledge FAPERJ and CNPq for the financial support.

REFERENCES

Anteneodo, C. and Plastino, A.R. (1999), "Maximum Entropy Approach to Stretched Exponential Probability Distributions", *J. Phys. A*.**32**, pp. 1089-1097.

Amato, I. (1997), "Candid Cameras for the Nanoworld", *Science* **276**, pp. 1982-1985.

Binnig, G., Quate, C.F. and Gerber, CH. (1986), "Atomic Force Microscope", *Phys. Rev. Lett.* **56**(9), pp. 930-933.

Franklin, J.N. (1970), "Well-posed Stochastic Extensions of Ill-Posed Linear Problems", *J. Math. Anal. Applications* **31**, pp. 682-716.

Frieden, B.R. (1972), "Restoring with Maximum Likelihood and Maximum Entropy", *J. Opt. Soc. Am.* **62**(4), pp. 511-518.

Glaeser, R.M. (1994), "Probing Toward Atomic Resolution in Molecular Topography*", Proc. Natl. Acad. Sci.USA* **91**, pp. 1981-1982.

Gull, S.F. and Daniell, G.J. (1978), "Image Reconstruction from Incomplete and Noisy data", *Nature* **272**(20), pp. 686-690.

Kang, M.G. and Katsaggelos, A.K. (1995), "General Choice of the Regularization Functional in Regularized Image Restoration", *IEEE Trans. Image Process.* **4**(5), pp.594-602.

Kapur, J.N. and Kesavan, H.K. (1992), "Entropy Optimization Principles with Applications", Academic Press Inc.

Karayiannis, N.B. and Venetsanopoulos, A.N. (1989), "Regularization Theory in Image Restoration: the Regularizing Operator Approach", *Optical Engineering* **28**(7), pp. 761-780.

Kokaram, A.C., Persad, N., Lasenby, J., Fitzgerald, W.J., Mckinnon, A. and Welland, M. (1995), "Restoration of Images from the Scanning-Tunneling Microscope", *Applied Optics* **34**(23), pp. 5121-5132.

Kress, R. (1989), "Linear Integral Equations" in "Applied Mathematical Sciences", vol. 82, Springer Verlay.

Mohammad-Djafari, A. and Demoment, G. (1985), "Image Restoration and Reconstruction using Entropy as a Regularization Functional" In "Maximum-Entropy and Bayesian Methods in Science and Engineering", vol. 2, Kluwer Academic Pub., pp. 341-355.

Oberleithner, H., Brinckmann, E., Schwab, A. and Krohne, G. (1994), "Imaging Nuclear Pores of Aldesterone-Sensisitive Kidney Cells by Atomic Force Microscopy", *Proc. Natl. Acad. Sci.USA* **91**, pp. 9784-9788.

Tikhonov, A.N. and Arsenin, V.Y. (1977), "Solutions of Ill-Posed Problems", Wiley, New York.

Wu, N. (1997), "The Maximum Entropy Method", Springer Series in Information Sciences.